

Robustness Threats of Differential Privacy

Nurislam Tursynbek
nurislam.tursynbek@gmail.com
Skolkovo Institute of Science and
Technology

Aleksandr Petiushko
petyushko.alexander1@huawei.com
Huawei Moscow Research Center

Ivan Oseledets
i.oseledets@skoltech.ru
Skolkovo Institute of Science and
Technology

ABSTRACT

Differential privacy is a powerful and gold-standard concept of measuring and guaranteeing privacy in data analysis. It is well-known that differential privacy reduces the model's accuracy. However, it is unclear how it affects security of the model from robustness point of view. In this paper, we empirically observe an interesting trade-off between the differential privacy and the security of neural networks. Standard neural networks are vulnerable to input perturbations, either adversarial attacks or common corruptions. We experimentally demonstrate that networks, trained with differential privacy, in some settings might be even more vulnerable in comparison to non-private versions. To explore this, we extensively study different robustness measurements, including FGSM and PGD adversaries, distance to linear decision boundaries, curvature profile, and performance on a corrupted dataset. Finally, we study how the main ingredients of differentially private neural networks training, such as gradient clipping and noise addition, affect (decrease and increase) the robustness of the model.

KEYWORDS

differential privacy, adversarial attacks, robustness, neural networks

1 INTRODUCTION

Although deep neural networks have achieved state-of-the-art performance in many complex problems and have been successfully applied to various real-world tasks, they appeared to be vulnerable to different kind of malicious attacks. These risks endanger the deployment of the models in some specific environments, such as medical image analysis [21] and video surveillance [42], where models have to be both secure and private. Adversaries might harm the systems by breaking the robustness of the neural network (security risks) or by inferring the secret information about the training data (privacy risks).

Data privacy attacks are based on the reverse engineering of the training process by using the model and its outputs to recover sensitive information about the training data. Numerous privacy attacks and their potential perils are described in the Related Work (Section 4). Differential privacy [13] is a powerful and gold-standard concept of measuring and guaranteeing privacy of data. It provides a rigorous framework, by efficiently bounding the influence of each individual input data, which allows differentially private algorithms to effectively handle against malicious attempts, by making few assumptions about the adversary's capabilities. According to the pioneering work of Dwork et al. [13], differential privacy provides a promise which claims that training data will not be affected, adversely or otherwise, no matter what other information is available elsewhere. This definition might first seemed to be too strict, but surprisingly recent studies figured out that anonymous data can

be robustly de-anonymized using other publicly available information, even in the case of large sparse datasets [2, 38]. Moreover, based on the definition, to preserve privacy of one sample in the training data, we should assume that the adversary has access to some or even all other samples from the training data. This scenario is not unreal, and can be observed, when the data is collected for example by means of crowdsourcing. To mitigate this issues during training of neural networks Abadi et al. [1] proposed a method to keep training data private, by introducing differential privacy to the learning procedure. This method protects individual privacy from strong adversaries, even with the full knowledge of the training procedure and model's hyperparameters, at the same time learning useful information about the dataset as a whole.

From security point of view, recently, researchers have discovered intriguing properties of neural networks [6, 50] of being brittle to adversarial examples [22]. Adversarial examples are specifically designed imperceptibly perturbed input data that completely fool neural network. In [22], adversarial examples were crafted using FGSM, which is a single-step procedure of perturbing input that maximally increases loss function. Adversarial examples have gained a significant attention as a tool of testing different properties of neural networks. Modified approaches, proposed to craft adversarial examples, are described in details in Section 2.3. Albeit many attacks are applied to digital data, further advances of them have been extended to physical world [30] and have brought serious security risks of using deep learning systems in the real world, especially in critical areas, such as self-driving cars [17], face identification systems [44], speech recognition technologies [8], compromising people's confidence in deep neural networks.

Several defense techniques that make neural networks robust or privacy-preserving were proposed recently. However, a typical defense techniques concentrate in one domain: either privacy-preservance or robustness, which still makes them unshielded and obscure in another. For instance, it is unclear how training procedure that guarantees privacy might affect the security (robustness) domain. As an example how differential privacy impacts a neural network model, the comparative illustration of normal cross-sections of the decision boundaries for differentially private and naturally trained classifiers is shown in Fig.1. The notable difference suggests that defending from privacy attacks also affect the underlying decision boundaries and robustness of model.

Differentially private training aims to enhance the privacy by clipping the individual per-example gradients and adding Gaussian noise for each of the update steps. The objective is to make the model invariant to the presence or absence of each sample in the training data, making impact of each data point less observable. Thus, intuitively, differential privacy have the potential to equalize (decrease or increase) the surrounding area (such as ℓ_p ball) of

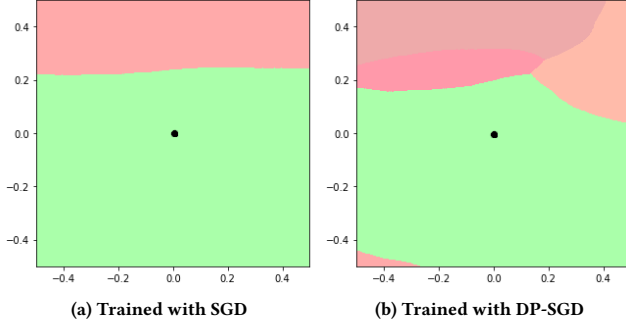


Figure 1: Random normal cross-sections of the decision boundary for CNN classifiers trained with SGD and DP-SGD on MNIST. The green region is correct class red regions are incorrect classes. The point at the center shows the sample. The classification regions are shown in the plane spanned by normal to the decision boundary (y-axis) and a random orthogonal direction (x-axis). Differential Privacy (DP-SGD) affects the underlying geometry of the decision boundaries.

samples for which model prediction is unchanged, making the model less or more robust.

In this work, we experimentally reveal the limitation of focusing solely on defending from privacy attacks with differential privacy, and its impact to the robustness to different perturbations.

The main contributions of this work are following:

- We experimentally demonstrate that differentially private models that strongly guarantee the privacy of the model and underlying training data can be more susceptible to adversarial examples and common corruptions.
- We study 5 different robustness measurements: accuracy drop of neural network after FGSM attack, robustness against PGD attack, distance to the closest decision boundary in ℓ_2 and ℓ_∞ , curvature profile of the decision boundary, performance on a corrupted dataset.
- We study how the main ingredients of differentially private training, such as gradient clipping and noise addition, affect the robustness.
- We test the hypothesis on the common benchmark using MNIST, MNIST-C, and CIFAR-10 datasets.

2 BACKGROUND

In this section we provide a theoretical background to adversarial examples and differentially private training.

2.1 Differential Privacy

Differential privacy [13] is a strong cryptographically-motivated mathematical concept of privacy guarantees. It quantifies how much information is leaked during a particular randomized mechanism and restricts the impact of any single sample of the dataset. Differential Privacy ensures that the model provides similar outputs for two adjacent datasets that differ only in a single entry (i.e. one

input-output sample is present in one dataset and absent in another). It is done by introducing the degree of randomness to the algorithm as a part of its logic.

DEFINITION 1 (RANDOMIZED ALGORITHM). An algorithm \mathcal{A} with domain \mathcal{D} and range \mathcal{R} is called a randomized algorithm, if for any input $d \in \mathcal{D}$, the output $\mathcal{A}(d) = r$ is drawn with probability $(\mathcal{A}(d))_r$ for each $r \in \mathcal{R}$. The probability space is defined as:

$$\mathcal{A} : \mathcal{D} \rightarrow \left\{ p \in \mathbb{R}^{|\mathcal{R}|} : \forall i; p_i \geq 0 \text{ and } \sum_{i=1}^{|\mathcal{R}|} p_i = 1 \right\}$$

DEFINITION 2 (DIFFERENTIAL PRIVACY). A randomized algorithm (or mechanism) $\mathcal{A} : \mathcal{D} \rightarrow \mathcal{R}$ with domain \mathcal{D} and range \mathcal{R} gives (\mathcal{E}, δ) -differential privacy ($\mathcal{E}, \delta > 0$), if for all datasets $D \in \mathcal{D}$ and $D' \in \mathcal{D}$, differing in at most one element, and for any subset of possible outputs $S \subseteq \mathcal{R}$, it is true that:

$$\Pr[\mathcal{A}(D) \in S] \leq e^{\mathcal{E}} \Pr[\mathcal{A}(D') \in S] + \delta$$

The privacy parameters \mathcal{E} and δ have the following interpretation: \mathcal{E} is a privacy budget (maximal privacy loss) of an algorithm, and δ (generally, $\delta < 1/|D|$), introduced in updated version [14], is the probability of possible violation of \mathcal{E} -differential privacy. The smaller the \mathcal{E} , the more private the model that is under investigation. Absolute privacy is observed when $\mathcal{E} = \delta = 0$, when nothing meaningful is learnt, aside from noise.

Differential privacy is widely used for measuring privacy and applying it to privacy-needed procedures, since it has several useful properties, which makes it attractive to deploy. One of them is that composition of differentially private components applied to the same (or overlapping) datasets is also differentially private. Also, differential privacy guarantees privacy for small groups of individuals, whose samples are correlated. Another property is the promise of guaranteeing that no matter what auxiliary information the adversary has, it will not impact on privacy. Furthermore, post-processing does not affect privacy guarantees of differentially private mechanism. All these properties are very suitable for the case of training neural networks. In this case the algorithm \mathcal{A} is the training procedure, which takes dataset D as input, learns from it with Stochastic Gradient Descent (SGD), and returns a model with hyperparameters as output. To make this mechanism differentially private, Abadi et al. [1] introduced an elegant approach called differentially private SGD (DP-SGD).

2.2 Differentially Private SGD [1]

To update parameters θ of a neural network to minimize the loss function \mathcal{L} , standard SGD approximates the gradient direction $-\nabla_{\theta} \mathcal{L}_{\theta}$ using a small, randomly chosen portion of it called batch. Usually, to make an algorithm random, the noise mechanism is added to the input, output, or the intermediate parts of the algorithm. In the case of SGD, adding noise to the input X or the model's parameters θ (output of the training procedure) would destroy the utility of learned model. To make the learning algorithm SGD differentially private, gradient noise was proposed [1]. Before noise addition, each individual component of the gradient is norm-clipped to bound the influence of each data point. Due to the lack of prior information about the norm of the gradients, each gradient

$\nabla \mathcal{L}_\theta(\theta, x_i)$ is clipped by ℓ_2 -norm, upper-bounded by threshold C . The full batch gradient is computed as a Gaussian noise with zero mean vector and covariance matrix $\sigma^2 C^2 \mathbf{I}$ added to the sum of each individual gradients, divided by the size of a batch. Procedure is summarized in Algorithm 1.

Algorithm 1 Differentially Private SGD [1]

INPUT: Dataset $\{(x_1, y_1), \dots, (x_N, y_N)\}$ batch size b , learning rate η , loss function $\mathcal{L}(\theta(x), y)$, T iterations, noise σ , clipping bound C

Initialize θ_0 randomly

for $t = 1$ to T **do**

 Sample random batch B_t of size b from a dataset

for $i = 1$ to b **do**

$$g_t(x_i) = \nabla \mathcal{L}_\theta(\theta, x_i)$$

$$\bar{g}_t(x_i) = \frac{g_t(x_i)}{\max(1, \frac{\|g_t(x_i)\|_2}{C})}$$

end for

$$\tilde{g}_t = \frac{1}{b} \left(\sum_{x_i \in B_t} \bar{g}_t(x_i) + \mathcal{N}(0, \sigma^2 C^2 \mathbf{I}) \right)$$

$$\theta_{t+1} = \theta_t - \eta \tilde{g}_t$$

end for

OUTPUT: Model θ_T and accumulated (\mathcal{E}, δ) -privacy loss

Abadi et al. [1] made an extensive research on quantifying privacy loss and invented a moments accountant method. The key principle of the moments accountant is to accumulate the privacy consumption by considering privacy loss as a random variable, and using its moment-generating functions to better understand that variable's distribution. For Gaussian noise used in the Algorithm 1, using notions from [15, Theorem 3.22], it was explicitly shown the relation between privacy parameters (\mathcal{E}, δ) and noise coefficient σ :

$$\sigma = \frac{\sqrt{2 \log \frac{1.25}{\delta}}}{\mathcal{E}} \quad (1)$$

Equipped with this background of SGD and DP-SGD, now we can explore how to compare their robustness to out-of-distribution examples.

2.3 Robustness Measurements to Adversarial Examples and Common Corruptions

Adversarial examples are perturbed input samples with well-designed small noise imperceptible to humans, that fool deep learning models, sometimes with very high confidence. These intriguing properties of neural networks were first discovered in [50], where authors described to create a small perturbations by solving an optimization problem:

$$\min_{\Delta} \|\Delta\|_p \quad \text{s.t.} \quad \arg \max_i \mathcal{F}_\theta(x + \Delta)_i \neq \arg \max_i \mathcal{F}_\theta(x)_i, \quad (2)$$

where $\mathcal{F}_\theta(\cdot)_i$ is the i -th output class of a classifier with parameters θ . Authors suggested to use L-BFGS optimization method to solve this problem. The topic has attracted a lot of attention, since a perturbation can be minimized in ℓ_p -norm (usually $p = 2$ or $p = \infty$) to very small values, invisible to a human eye.

2.3.1 FGSM. Goodfellow et al. [22] proposed an efficient single-iteration method, using backpropagation, to compute an ℓ_∞ -bounded adversarial perturbation for a given input x called Fast Gradient Sign Method (FGSM):

$$x_{adv} = x + \varepsilon \text{sign}(\nabla_x \mathcal{L}(\theta, x, y)), \quad (3)$$

where y is the true class of input x , θ is the model parameters, $\nabla_x \mathcal{L}(\theta, x, y)$ computes the gradient of a cost function with respect to x . FGSM serves as a simple, yet effective, way of testing robustness of a neural network.

2.3.2 PGD. Following FGSM, a straightforward iterative extension of it was found to be successful in [30, 31]. Madry et al. [34] indicated, that this is equivalent to ℓ_∞ version of standard large-scale constrained optimization method, called Projected Gradient Descent (PGD). PGD begins with $x_{adv}^0 = x$ and then iteratively updates with a step-size α in the direction of the signed gradient $\text{sign}(\nabla_x \mathcal{L}(\theta, x_{adv}^t, y))$ of the loss function with respect to input, whose value at iteration t is x_{adv}^t :

$$x_{adv}^{t+1} = \text{Clip} \{x_{adv}^t + \alpha \text{sign}(\nabla_x \mathcal{L}(\theta, x_{adv}^t, y)), x - \varepsilon, x + \varepsilon\} \quad (4)$$

It should be mentioned, that after each update, the input is additionally clipped to have proper input bounds, like image pixel constraints. In [34], authors mention that PGD-based attacks are the main tool to construct adversarially trained models, which are defended models trained on adversarial examples instead of clean samples. It was discovered that signed gradients produce better adversarial attacks compared to raw gradients in the updating rule of PGD.

2.3.3 DeepFool. A simple and accurate method to compute an adversarial example to an input is DeepFool [35]. DeepFool is a few-step method to compute a more optimized adversarial perturbation to the input, compared to FGSM. Authors elegantly propose to use a geometric trick to locally linearize decision boundaries using Taylor expansion and then to compute a distance to the closest boundary. That distance in the space of inputs is a perturbation needed to add to the input to make it adversarial example. The method is applicable to ℓ_2 and ℓ_∞ bounded perturbations. The closest ℓ_2 distance from a data sample x with a true class to a boundary of any class k is approximated by:

$$l_k(x) = \frac{|f_{true}(x) - f_k(x)|}{\|\nabla_x f_{true}(x) - \nabla_x f_k(x)\|_2} \quad (5)$$

The closest ℓ_∞ distance is approximated by:

$$l_k(x) = \frac{|f_{true}(x) - f_k(x)|}{\|\nabla_x f_{true}(x) - \nabla_x f_k(x)\|_1} \quad (6)$$

Here, $f_k(x)$ is the output of predicted logits, corresponding to the k -th class and $\nabla_x f_k(x)$ is its gradient with respect to input x . The closest distance to wrong (adversarial) class is computed as $\min_{k \neq \text{true}} l_k(x)$.

2.3.4 CURE. Moosavi et al. [36] discovered that curvature of the decision boundaries of a neural network classifier is inversely proportional to its robustness. It was empirically demonstrated that decision boundaries of adversarially trained (defended) models are less curved, compared to undefended models, and it was proposed to use the curvature regularization (CURE) as an alternative to the

adversarial training. The curvature profile with respect to inputs of a loss function is suggested to compute as eigenvalues of a Hessian matrix:

$$H = \left(\frac{\partial^2 \mathcal{L}}{\partial x_i \partial x_j} \right) \in \mathbb{R}^{d \times d} \quad (7)$$

Here, $x \in \mathbb{R}^d$ is considered as a flattened version of input. Curvature profile is mostly consisted of zero eigenvalues, but might be positive and negative as well.

2.3.5 MNIST-C. Recently, a corrupted version of MNIST was introduced as MNIST-C [37], which serves as an out-of-distribution robustness benchmark for computer vision models. Dataset contains 31 corruptions of different types applied to the standard MNIST [32], which still preserves semantic content of an underlying image, however significantly degrades the accuracy of a model, even if the model is adversarially defended, indicating tendency that adversarial robustness is not transferable to robustness against common corruptions.

3 EXPERIMENTAL STUDY

In this section, we describe the experimental evaluations of different robustness measurements for models trained with SGD and DP-SGD. Following [1], we perform experiments on the standard MNIST dataset, since its easier and fast to train models on it. We also perform some experiments on CIFAR-10 dataset. This datasets are public and serve as a benchmark for different machine learning tasks. In all experiments we use Pytorch framework and NVidia GeForce GTX GPUs.

For experiments with MNIST dataset, which contains 60000 training and 10000 testing gray-scale images of size 28×28 [32], we used a neural network architecture which consists of two convolutional layers with kernel size 5×5 , stride 1, and number of channels 20 and 50, with 2×2 max-pooling, following by two fully-connected layers with 500 hidden units each. The activation function is ReLU for all layers. We set the learning rate 0.05, and train networks for 50 epochs. The batch size is set to be 256. For the fair comparison, we do not change experimental settings for all cases. In subsections 3.2, 3.3, 3.4 and 3.5, we use the noise value $\sigma = 1.3$ and the clipping bound $C = 1.0$ in case of DP-SGD.

3.1 Robustness Measurement with FGSM

As it was mentioned, FGSM significantly decreases the accuracy of the undefended model depending on the ℓ_∞ -bound of the perturbation ϵ , pointing that standard neural networks trained with SGD are not robust to simple adversarial example. Surprisingly, the models trained with DP-SGD can be even more non-robust, i.e. the accuracy for these models decrease quicker. Figure 2 demonstrates the plots of accuracies depending on perturbation ℓ_∞ -norm ϵ . One might expect that the accuracy drop would be similar for different training procedures, but DP-SGD decreases faster, increasing initial gap 2.6% between accuracies, sometimes, reaching 15.4% for $\epsilon = 0.12$, and always more than initial value. More swift accuracy drop of classifier trained with DP-SGD indicates that DP-SGD reduces robustness to FGSM adversarial examples. Moreover, to decrease performance to the same level of accuracy for DP-SGD requires weaker adversary.

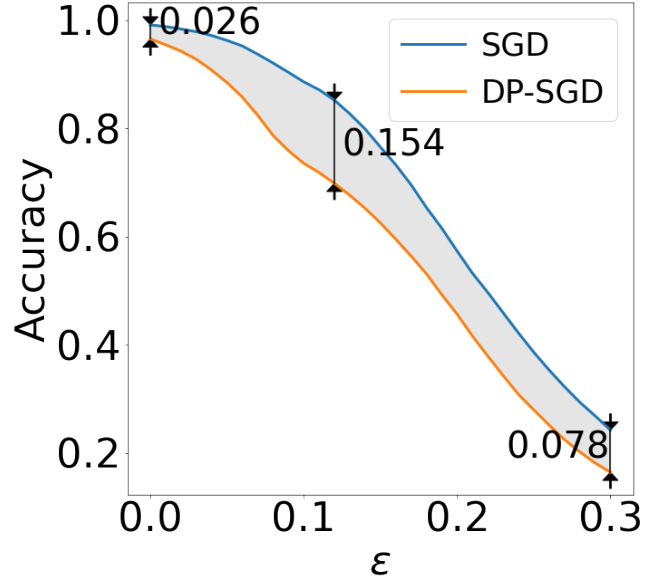


Figure 2: Decrease of accuracy with increasing strength of adversary for neural networks trained with SGD and DP-SGD. Here ϵ is adversary’s strength (ℓ_∞ of perturbation) for MNIST

For the case of DP-SGD, we used the noise value $\sigma = 1.3$ and the clipping bound $C = 1.0$. These values, according to equation (1), for $\delta = 10^{-6}$ give privacy budget $\epsilon < 5$. The next step is to explore the dependence of two main ingredients of DP-SGD: gradient clipping and noise addition. In Fig.3 we show the dependence of accuracy curves for different ℓ_∞ of perturbation ϵ for models with varying noise σ and clipping bound C .

In Figure 3a, the gap between standard and private training is increasing with the increase of the noise coefficient σ , which means that more private (noisy) algorithms are less robust. Figure 3b shows the dependence of FGSM curves on the clipping bound C . Since the coefficient C also appears in noise (Algorithm 1), it also decreases robustness by increasing the accuracy gap even faster. This is done in order to add noise comparable to the norm of the clipped gradients. For this reason, we would like to explore how pure clipping affects accuracies. For this task we vary C only for clipping the norm of gradients, while keeping the noise as $\mathcal{N}(0, \sigma^2 \mathbf{I})$, not $\mathcal{N}(0, \sigma^2 C^2 \mathbf{I})$. The results are shown in Figure 3c and indicate that the smaller clipping value is less robust and less accurate. This implies that more private models that bounds individual gradients to smaller values are less robust.

3.2 Robustness Measurement with PGD

As it was pointed out in [34], the PGD attack finds local maxima of the loss function, based on the constrained the adversary has, and serves as “universal” adversary among first-order approaches. We can use this information to compare robustness of a neural network.

First, we compare accuracy of the network when PGD attack is applied for a fixed number of steps and adversary’s strength ϵ . The

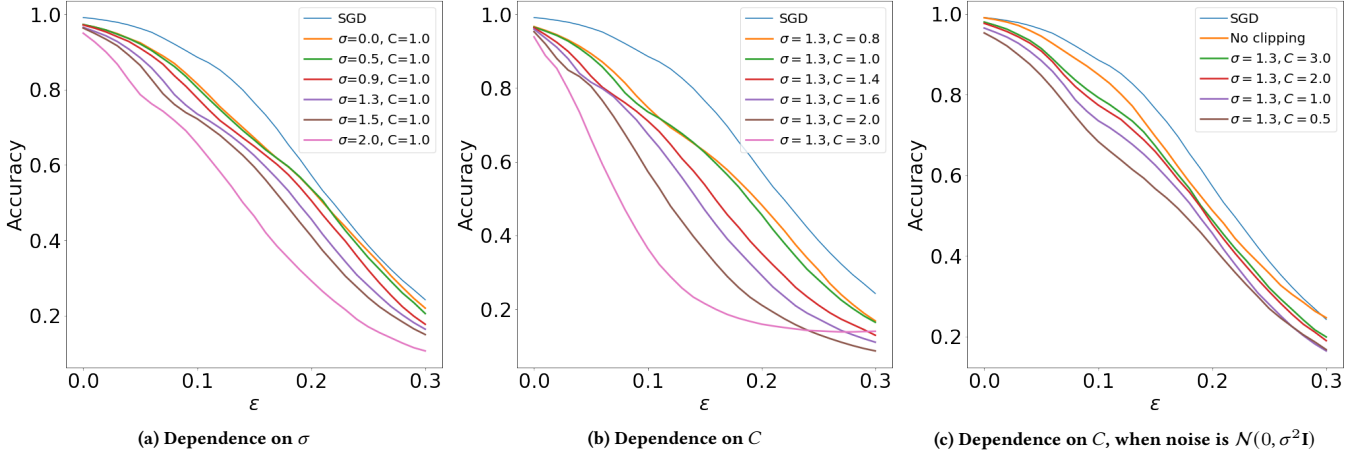


Figure 3: Dependence of FGSM accuracy curves on the noise and clipping bound parameters for MNIST.

PGD settings	SGD Acc.	DP-SGD Acc.	Difference
$\epsilon = 0.3, steps = 40$	1.00%	0.23%	0.77%
$\epsilon = 0.2, steps = 40$	10.15%	4.36%	5.79%
$\epsilon = 0.1, steps = 40$	80.44%	60.89%	19.55%
$\epsilon = 0.3, steps = 30$	3.06%	1.38%	1.68%
$\epsilon = 0.2, steps = 30$	15.84%	7.88%	7.96%
$\epsilon = 0.1, steps = 30$	80.63%	61.10%	19.53%

Table 1: PGD Results for MNIST.

results are shown in Table 1 and indicate that for $\epsilon = 0.1; 0.2$, the gap between SGD and DP-SGD increases compared to initial gap 2.6%, which indicates that DP-SGD trained network can be less robust to adversaries with small strength.

Next, we compare a number of iterations to reach an adversarial class for a particular adversarial strength ϵ . The comparative illustration is shown in Figure 4 for different step-sizes α , in case when adversarial strength $\epsilon = 0.1; 0.2; 0.3$. For the small ϵ , it might be the case that adversary does not find adversarial class. Less number of iterations needed for PGD to fool the network with DP-SGD training indicates that DP-SGD might reduce robustness to PGD adversarial examples.

3.3 Robustness Measurement as Distance to Closest Decision Boundary

In [35] it was proposed to linearly approximate decision boundaries of neural networks and to compute an optimized perturbation as a vector, directed to the closest decision boundary, whose magnitude is the distance to this boundary. To calculate ℓ_2 and ℓ_∞ magnitudes to decision boundaries, we use equations (5) and (6) for all test samples. Then, the constructed histogram of distances is shown in Figure 5a and 5b. It should be mentioned, that distances are only computed for inputs with true predicted values.

As it can be seen from the histograms in Figure 5a and 5b, the decision boundaries of the model trained with DP-SGD is closer

to data samples. When using the DP-SGD, the average value for ℓ_∞ -bounded closest distance is reduced from 0.154 to 0.131 (~ 15% drop) and ℓ_2 -bounded closest distance is reduced from 1.965 to 1.654 (~ 16% drop). Reduction in distance to the closest decision boundary might indicate that DP-SGD under these settings builds a boundary that is close to data samples, which makes the model more susceptible to DeepFool adversarial examples (or less robust in other words).

3.4 Robustness Measurement as Curvature Profile

In Figure 1 the random normal cross-section of the decision boundary for a CNN classifier is shown. The decision boundary of the classifier trained with DP-SGD is not only close to sample as shown in Section 3.3, but also "looks more curved" compared to the the decision boundary of the classifier trained with SGD. According to the recent finding in [36], more robust models have less curved (more "linear") decision boundaries, and vice versa.

To quantitatively measure the curvature profile of the network, following [36], we compute the curvature profile as sorted eigenvalues of Hessian matrix with respect to input data (Equation (7)) at 100 random test samples, and show the average curvature in Figure 5c. Since most of the eigenvalues are close to 0, to better understand curvature profiles, we plot a logarithmic-scaled largest 15 eigenvalues. As shown in Figure 5c, curvature profile of the model trained with DP-SGD has higher eigenvalue magnitudes (the largest eigenvalue difference is 100 times), which indicates that the model trained with DP-SGD under these settings produces more curved decision boundaries, and thus, according to [36], makes it less robust to adversarial examples.

3.5 Robustness Measurement to Common Corruptions

Common corruptions also can be considered as a robustness benchmark. These corruptions were initially proposed in [25], and the

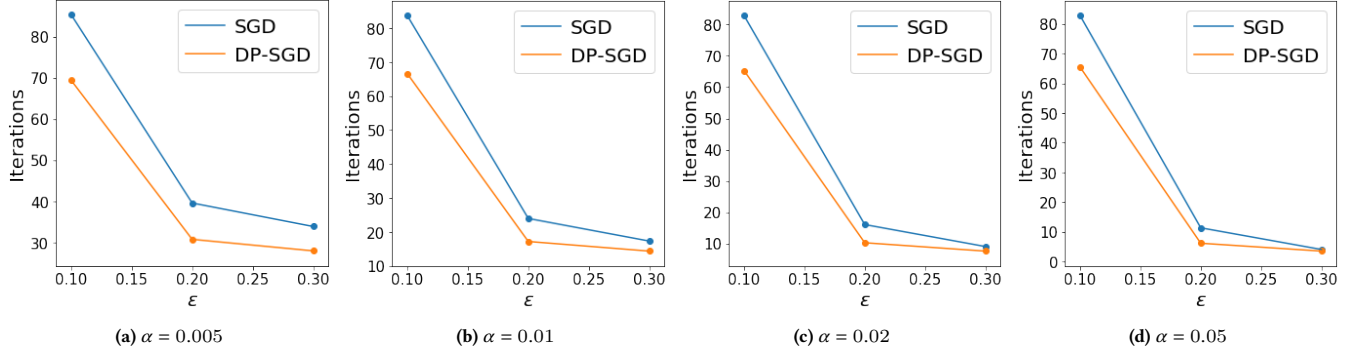


Figure 4: Number of PGD iterations, needed to achieve adversarial class for MNIST.

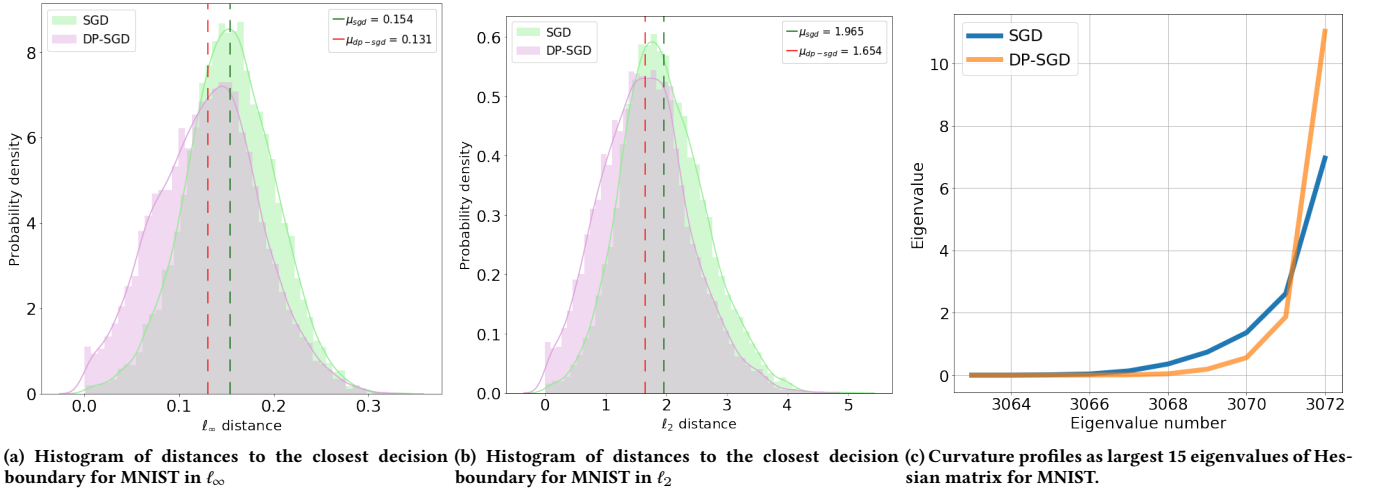


Figure 5: Distances and curvature results of MNIST experiments.

extension to MNIST was recently introduced in [37]. Here, we describe the results of evaluation of neural networks trained with SGD and DP-SGD for the robustness benchmark MNIST-C.

The results are shown in Table 2. They clearly indicate that differential privacy has significant impact on model’s robustness to common corruptions. The initial baseline difference gap between SGD and DP-SGD model of 2.61% increases for almost all corruptions and in average it increases to 15.99%, sometimes reaching extremely large gaps of 69.09%, 64.57%, 63.47%. The largest gaps are produced for Brightness, Fog and Frost corruptions, which is interesting, because visually these three corruptions are also similar to each other. We also show evaluations on MNIST-C dataset for different values of DP-SGD parameters σ and C . Results in Table 2 indicate that increasing C for the same σ as well as increasing σ for the same C leads to increasing the accuracy drop between corrupted and not corrupted dataset.

3.6 Experiments with CIFAR-10

For experiments with CIFAR-10 dataset, which contains 50000 training and 10000 testing colour images of size $32 \times 32 \times 3$, similarly to [1, 29], we used a neural network architecture which consists of two convolutional layers followed by three fully-connected layers. The convolutional layers use 3×3 convolutions with stride 1, followed by ReLU activation and max-pooling of kernel size 3×3 with a stride 2. The flattened output of the second convolutional layer is then passed to three fully-connected layers with 500 hidden units each, and ReLU activation. Computing per-example gradients is computationally expensive procedure, thus, we pre-train convolutional layers on the CIFAR-100 dataset that has similar parameters to CIFAR-10, except that images are classified into 100 classes. Moreover, it was previously shown that parameters of convolutional layers learned from one dataset often can be used on another one without retraining on another [26]. We train only the fully connected layers with this architecture in both SGD and DP-SGD cases. Learning rate is 0.01, batch size is 200 and number of epoch is 200.

Corruption	SGD	DP-SGD ($\sigma = 1.3, C = 1$)	Difference		$\sigma = 1.3, C = 0.8$	$\sigma = 1.3, C = 1.2$	$\sigma = 0.7, C = 1$	$\sigma = 1.5, C = 1$
Baseline	99.14	96.53	2.61		96.67	96.56	97.22	96.34
Brightness	96.71	27.62	69.09		32.22	22.54	36.43	23.5
Fog	91.59	27.02	64.57		29.68	24.8	33.12	24.95
Impulse Noise	95.34	89.43	5.91		90.41	88.24	91.78	88.39
Rotate	92.77	84.34	8.43		84.15	83.87	85.14	83.28
Shot Noise	98.06	95.09	2.97		95.15	94.66	95.93	94.46
Translate	56.32	30.98	25.34		30.74	30.32	33.32	29.25
Canny Edges	69.89	63.64	6.25		65.89	62.04	67.62	62.6
Glass Blur	95.97	90.63	5.34		90.82	90.32	91.91	90.12
Scale	94.98	71.72	23.26		70.33	71.4	75.07	69.98
Spatter	97.12	94.13	2.99		94.2	93.86	95.06	93.6
Zigzag	88.09	80.03	8.06		80.37	79.46	82.33	79.08
Dotted Line	96.88	94.13	2.75		94.07	93.51	94.97	93.42
Motion Blur	95.91	85.91	10.00		84.7	86.18	87.29	85.4
Shear	97.84	91.16	6.68		91.4	91.01	92.76	90.58
Stripe	88.05	62.39	25.66		61.41	61.33	66.6	59.45
Contrast	95.57	71.66	23.91		77.5	65.79	84.34	66.61
Defocus Blur	95.66	88.96	6.70		88.94	88.97	90.05	88.77
Frost	94.05	30.58	63.47		33.98	27.84	38.66	28.11
Gaussian Blur	87.80	83.09	4.71		82.81	83.09	82.12	83.39
Gaussian Noise	88.05	81.21	13.33		82.69	79.94	85.07	80.16
Pessim Noise	92.65	92.41	0.24		93.18	91.42	93.54	91.68
Pixelate	97.94	94.18	3.76		94.19	93.93	95.42	93.62
Saturate	98.39	83.99	14.40		84.61	83.49	87.32	82.66
Speckle Noise	98.33	95.57	2.76		95.48	95.15	96.14	95.03
Zoom Blur	98.02	91.41	6.55		91.6	91.25	93.12	90.94
Jpeg Compression	99.09	96.52	2.57		96.29	96.32	97.05	96.1
Elastic Transform	86.73	72.0	14.73		71.31	71.65	74.0	70.78
Quantize	98.98	96.33	2.65		96.25	96.12	96.82	95.88
Line	85.56	82.53	3.03		82.6	81.71	84.16	81.45
Inverse	37.27	9.54	27.73		9.20	9.59	8.54	9.54
Snow	96.33	58.22	38.11		60.11	56.95	64.48	56.38
Average	90.72	74.73	15.99		75.36	73.77	77.42	73.52

Table 2: MNIST-C Results

The standard non-private SGD training in this settings is able to reach test accuracy 81.3%, while the differentially private SGD with $\sigma = 1$ and $C = 3$ is able to reach the test accuracy 70.1%. The large gap 11.2% between two models on the baseline not perturbed CIFAR-10 dataset makes comparison of the robustness with adversarially perturbed (FGSM, PGD) and commonly corrupted samples uninformative. In case of CIFAR-10, we measure and compare the robustness as the distance to the closest decision boundary and as a curvature profile.

In Figures 6a and 6b, the results for distances to the closest decision boundary are shown. Similarly to Section 3.3, the decision boundaries for DP-SGD is closer to samples. With the addition of differential privacy, the average value for ℓ_∞ -bounded closest distance is reduced from 0.268 to 0.238 ($\sim 11.2\%$ drop) and ℓ_2 -bounded closest distance is reduced from 0.178 to 0.158 ($\sim 11.2\%$ drop). The smaller distance to the closest decision boundary might indicate

that the DP-SGD model is more susceptible to DeepFool adversarial examples (less robust).

Similarly to experiments in Section 3.4, we compute the curvature profile as the largest 10 eigenvalues of Hessian matrix with respect to input data (Equation (7)) at 100 random test samples, and show the average curvature in Figure 6c. Although not all eigenvalues for DP-SGD are higher than SGD, the largest and the most important eigenvalue of the DP-SGD trained model is higher, which indicates that model trained with DP-SGD under these settings produces more curved decision boundaries, thus according to [36] makes it less robust to adversarial examples.

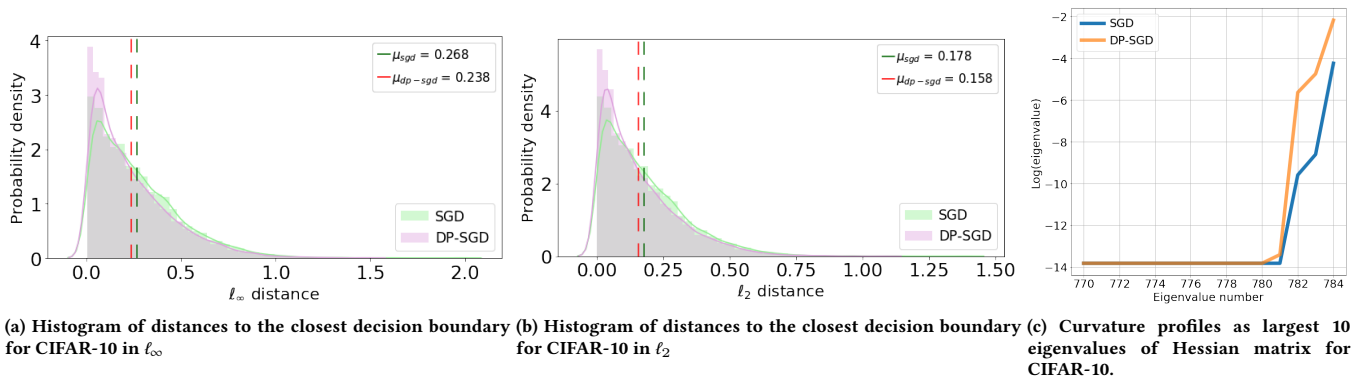


Figure 6: Results of CIFAR-10 experiments.

4 DISCUSSION AND RELATED WORK

From privacy point of view, some information is considered to be sensitive and secret, while an adversary targets to obtain that private information about the model’s underlying training data or the model itself. Model privacy has been found to be violated, by showing the existence of several malicious approaches: restoring model details with model extraction attacks [51], stealing the hyper-parameters of the model [52], intentionally exploiting back-doors to the model to make it less private [47]. Another type of privacy attacks, data privacy attacks, are using model and its outputs to recover sensitive information about the training data. One of them is the membership inference attack [46], where an attacker aims to identify whether a particular data point was a part of a training dataset or not. The threat from this type of attacks is clear in scenarios, such as health analytics, where the difference between case and control groups can leak patient’s personal conditions. Privacy attacks also include the learning global properties of private training data [20], inferring missing information using a model and incomplete information [19], obtaining meaningful data from models [3]. Another important privacy attack is the model inversion attack [18], where an adversary aims to approximate some of the model’s training data points, using some intermediate layers output, or even using only outputs of the model. In [18], the model inversion attack has been applied to a face classification model, that allowed to reconstruct recognizable faces from training data using only a certain output class.

Data privacy attacks become even more successful when the training dataset has a small number of samples, like in medical data analysis, indicating model’s overfitting to them [53]. The connection of privacy attacks to model overfitting was studied in [53], where authors show that overtraining of neural networks leads to more privacy risks. Later, the unintended memorization have been discovered in [7], where authors showed that some points of training data can be easily recovered from the model that is not overfitted towards training data, nevertheless memorized some specific unique information. Usually these unique corner samples are extremely privacy sensitive and contain personal secret details. For example, authors of [7] have shown the threat of recovering Social

Security Numbers from text completion neural network trained on millions of email users.

To mitigate these privacy issues, several approaches to defend private information were proposed [1, 24, 39, 45]. In [39], the adversarial regularization was proposed to protect membership privacy. In [24, 45], authors proposed to secure multi-party machine learning systems by the adversarial training on contamination attacks [24] or paralleling the optimization algorithms [45]. Abadi et al. [1] proposed to apply the differential privacy [13] to the learning procedure, which efficiently bounds the influence of each input data point to a mechanism’s output. Differential privacy has been used in many classical machine learning algorithms to reduce privacy leakage of the training data [5, 9, 10, 16, 28, 43, 49, 54]. Abadi et al. [1] additionally proposed privacy accounting method to quantify privacy loss of the training mechanism.

Though this powerful technique successfully protects data samples from privacy attacks, as shown in [1], the accuracy of differentially private models is less in comparison to undefended models. Moreover, Bagdasaryan et al. [4] recently discovered that it has significant impact on model’s accuracy, by showing that reduction of accuracy and gaining in privacy are not borne equal. They showed that models trained with DP-SGD not only have less accuracy, but also have significantly less fairness for underrepresented classes. Authors demonstrated that DP-SGD trained gender classification model exhibits much lower accuracy for black people compared to white people, which identifies the model’s additional unfairness. The intuitive explanation is the following: as underrepresented groups imply larger gradients, thus clipping and random noise reduce their influence on the model.

Several other works used concept of privacy and adversarial robustness in their studies [12, 23, 27, 33, 41, 48].

Lecuyer et. al [33] proposed to use concepts of differential privacy to certify adversarial robustness of the model. They certify a prediction of the neural network with additive Gaussian noise to input data at test time and guarantee prediction label at some surrounding area for each sample.

In [12], it was proposed to detect anomalies and backdoor poisoning attacks to a model via differential privacy. Authors train autoencoders in differentially private setting, by the similar per-example

gradient clipping and noise addition, and use loss thresholds to detect anomalies and poisoning attacks.

In [27], a defensive methodology from the black-box membership inference attacks using adversarial examples was proposed. Their algorithm randomly adds noise to the confidence score vector predicted by the target classifier to transform a data sample into an adversarial example.

Similar to our work, but other way around, a research was recently done in [48], where authors studied the unexpected privacy risks of securing models to adversarial examples. They showed that models trained with different adversarial training techniques are more vulnerable to the membership inference attack, which indicates that focusing solely on adversarial defense has impact on leakage of private information. Intuitively, they explain that adversarial defense strategy tries to robustify the model by making sure that outputs of ℓ_p -ball around training data points remains unchanged, which leaks even more information about its membership during training process.

Following [48], theoretical analysis of the connection between the adversarial training and membership inference attacks was performed in [23]. Authors proposed the theoretical and experimental framework to compare the standard and adversarially robust training methods from the membership privacy point of view. However, authors did not study 'reverse' problem of the effect of differential privacy to the robustness of the model.

Phan et al. [41] proposed to use the adversarial training with differential privacy, but only briefly mentioned without proof the interplay trade-off between adversarial robustness and privacy of the model. We, on the other hand, experimentally show that differential privacy (under some settings) indeed reduces the model's robustness to adversarial examples and common corruptions.

Taking into consideration the related works above and observations of this paper (Section 3), a principle question arises naturally:

Is this trade-off a fundamental problem?

It is hard to find a solid mathematical answer if differential privacy and robustness of a model are always necessarily in conflict. On one hand, there is no explicit connection between training models with differential privacy and decreasing model's robustness.

On the other hand, results of Section 3 empirically show that differential privacy (under some settings) decreases model's robustness to adversarial examples and common corruptions. Intuitive explanation for this effect is the following: training with differential privacy consists of clipping the individual per-example gradients and adding Gaussian noise to them for each of the update steps. It makes a model invariant to the existence of each sample in the training data, making impact of the samples to the model less observable. Therefore, differential privacy potentially tends to equalize (decrease or increase) the surrounding area (such as ℓ_p ball) of samples for which model prediction is unchanged, making overall the model less or more robust to different perturbations.

The difficulty of judgement the fundamentality of the privacy-robustness trade-off was also discussed in [48], where authors empirically demonstrated the privacy risks of securing models against adversarial examples. The mathematical formulation of the trade-off between adversarial training and membership inference was

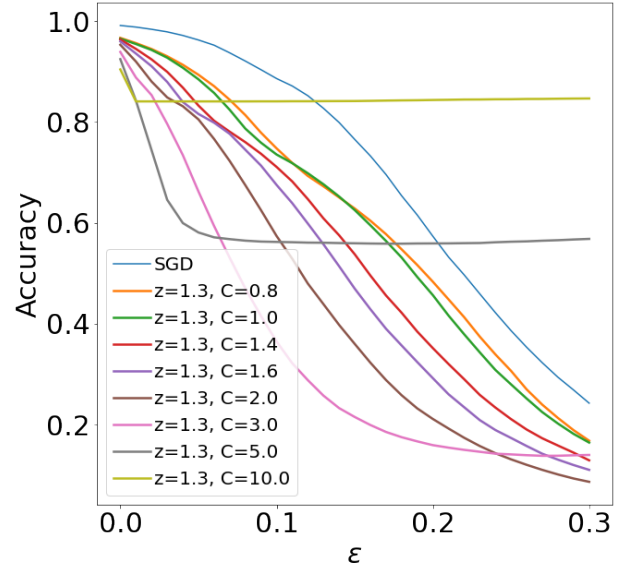


Figure 7: Dependence of FGSM accuracy curves on clipping bound for MNIST

done in [23]. Authors proved that an adversarially trained model can either be more or less susceptible to the membership inference attack than a standard model, showing there exist settings with and without privacy-robustness trade-off. The settings are conditioned on ℓ_p -ball radius ϵ used in the adversarial training, and training size n .

All the experiments in the Section 3 demonstrate settings, under which differential privacy decreases robustness of the model. However, in Figure 3b, we see that for the sufficiently big clipping bound ($C = 3.0$), there is an effect of 'plateau' in terms of adversarial robustness with strong FGSM adversaries (big magnitude of ℓ_∞). Increasing the magnitude of the clipping bound C to even larger value, we unexpectedly got the surprising results: the 'plateau' accuracy line goes higher as the clipping bound C increases. Figure 7 demonstrates that surprising effect of settings when differential privacy helps improving robustness of the model to FGSM adversaries.

The results in Figure 7 support findings in [23], that there exist some settings, when there is no conflict between privacy and robustness, and, moreover, improving one might also positively affect another. The increase of robustness with increasing C is primarily due to the existence of C in the gradient noise term (the gradient noise in DP-SGD is $\mathcal{N}(0, \sigma^2 C^2 \mathbf{I})$). Gradient noise have been found to improve learning for very deep networks [40]. Authors assert that gradient noise helps the model to explore the optimization landscape, escaping saddle points and local minima, possessing attractive robustness properties. Another possible explanation is, perhaps, training with big gradient noise has some connection to randomized smoothing [11] when big noise is added to the input during training process, which guaranteed to certify adversarial robustness of the model.

5 CONCLUSION

It is well-known that neural networks trained with standard gradient descent methods, such as SGD, are brittle and not secure to different out-of-distribution examples. In this paper, we experimentally demonstrated that models, trained by differentially private SGD, that strongly protects the privacy of the model and underlying training data, might be even less secure, i.e. more susceptible to adversarial examples and common corruptions. In our experiments, we studied five different robustness measurements: accuracy drop after a single FGSM attack, robustness against PGD attack and a number of iterations to achieve adversarial class, distance to the closest decision boundary in ℓ_2 and ℓ_∞ , curvature profile of the decision boundary and performance on a corrupted dataset. We also studied how the main components of differentially private training (gradient clipping and noise addition) affect the robustness. The results indicate, that differential privacy reduces not only model's accuracy, but also affect the robustness of the model, decreasing or increasing. This threatens differential privacy to be deployed in security-critical scenarios. Interesting effect is observed with big gradient noise, when privacy and robustness are not in conflict. This effect and solid mathematical explanation of connection between differential privacy and robustness are the perspective directions for the future work.

REFERENCES

- [1] Martin Abadi, Andy Chu, Ian Goodfellow, H Brendan McMahan, Ilya Mironov, Kunal Talwar, and Li Zhang. 2016. Deep learning with differential privacy. In *Proceedings of the 2016 ACM SIGSAC Conference on Computer and Communications Security*. 308–318.
- [2] Charu C Aggarwal. 2005. On k-anonymity and the curse of dimensionality. In *Vldb*, Vol. 5. 901–909.
- [3] Giuseppe Ateniese, Giovanni Felici, Luigi V Mancini, Angelo Spognardi, Antonio Villani, and Domenico Vitali. 2013. Hacking smart machines with smarter ones: How to extract meaningful data from machine learning classifiers. *arXiv preprint arXiv:1306.4447* (2013).
- [4] Eugene Bagdasaryan, Omid Poursaeed, and Vitaly Shmatikov. 2019. Differential privacy has disparate impact on model accuracy. In *Advances in Neural Information Processing Systems*. 15453–15462.
- [5] Raef Bassily, Adam Smith, and Abhradeep Thakurta. 2014. Private empirical risk minimization: Efficient algorithms and tight error bounds. In *2014 IEEE 55th Annual Symposium on Foundations of Computer Science*. IEEE, 464–473.
- [6] Battista Biggio, Igino Corona, Davide Maiorca, Blaine Nelson, Nedin Šrđić, Pavel Laskov, Giorgio Giacinto, and Fabio Roli. 2013. Evasion attacks against machine learning at test time. In *Joint European conference on machine learning and knowledge discovery in databases*. Springer, 387–402.
- [7] Nicholas Carlini, Chang Liu, Jernej Kos, Ulfar Erlingsson, and Dawn Song. 2018. The secret sharer: Measuring unintended neural network memorization & extracting secrets. *arXiv preprint arXiv:1802.08232* (2018).
- [8] Nicholas Carlini and David Wagner. 2018. Audio adversarial examples: Targeted attacks on speech-to-text. In *2018 IEEE Security and Privacy Workshops (SPW)*. IEEE, 1–7.
- [9] Kamalika Chaudhuri, Claire Monteleoni, and Anand D Sarwate. 2011. Differentially private empirical risk minimization. *Journal of Machine Learning Research* 12, Mar (2011), 1069–1109.
- [10] Kamalika Chaudhuri, Anand D Sarwate, and Kaushik Sinha. 2013. A near-optimal algorithm for differentially-private principal components. *The Journal of Machine Learning Research* 14, 1 (2013), 2905–2943.
- [11] Jeremy M Cohen, Elan Rosenfeld, and J Zico Kolter. 2019. Certified adversarial robustness via randomized smoothing. *arXiv preprint arXiv:1902.02918* (2019).
- [12] Min Du, Ruoxi Jia, and Dawn Song. 2019. Robust Anomaly Detection and Backdoor Attack Detection Via Differential Privacy. *arXiv preprint arXiv:1911.07116* (2019).
- [13] Cynthia Dwork. 2008. Differential privacy: A survey of results. In *International conference on theory and applications of models of computation*. Springer, 1–19.
- [14] Cynthia Dwork, Krishnaram Kenthapadi, Frank McSherry, Ilya Mironov, and Moni Naor. 2006. Our data, ourselves: Privacy via distributed noise generation. In *Annual International Conference on the Theory and Applications of Cryptographic Techniques*. Springer, 486–503.
- [15] Cynthia Dwork, Aaron Roth, et al. 2014. The algorithmic foundations of differential privacy. *Foundations and Trends® in Theoretical Computer Science* 9, 3–4 (2014), 211–407.
- [16] Cynthia Dwork, Guy N Rothblum, and Salil Vadhan. 2010. Boosting and differential privacy. In *2010 IEEE 51st Annual Symposium on Foundations of Computer Science*. IEEE, 51–60.
- [17] Kevin Eykholt, Ivan Evtimov, Earlene Fernandes, Bo Li, Amir Rahmati, Chaowei Xiao, Atul Prakash, Tadayoshi Kohno, and Dawn Song. 2018. Robust physical-world attacks on deep learning visual classification. In *Proceedings of the IEEE Conference on Computer Vision and Pattern Recognition*. 1625–1634.
- [18] Matt Fredrikson, Somesh Jha, and Thomas Ristenpart. 2015. Model inversion attacks that exploit confidence information and basic countermeasures. In *Proceedings of the 22nd ACM SIGSAC Conference on Computer and Communications Security*. 1322–1333.
- [19] Matthew Fredrikson, Eric Lantz, Somesh Jha, Simon Lin, David Page, and Thomas Ristenpart. 2014. Privacy in pharmacogenetics: An end-to-end case study of personalized warfarin dosing. In *23rd {USENIX} Security Symposium ({USENIX} Security 14)*. 17–32.
- [20] Karan Ganju, Qi Wang, Wei Yang, Carl A Gunter, and Nikita Borisov. 2018. Property inference attacks on fully connected neural networks using permutation invariant representations. In *Proceedings of the 2018 ACM SIGSAC Conference on Computer and Communications Security*. 619–633.
- [21] Mahadevan Gomathisankaran, Xiaohui Yuan, and Patrick Kamong. 2013. Ensure privacy and security in the process of medical image analysis. In *2013 IEEE International Conference on Granular Computing (GrC)*. IEEE, 120–125.
- [22] Ian J Goodfellow, Jonathon Shlens, and Christian Szegedy. 2014. Explaining and harnessing adversarial examples. *arXiv preprint arXiv:1412.6572* (2014).
- [23] Jamie Hayes. 2020. Provable trade-offs between private & robust machine learning. *arXiv preprint arXiv:2006.04622* (2020).
- [24] Jamie Hayes and Olga Ohrimenko. 2018. Contamination attacks and mitigation in multi-party machine learning. In *Advances in Neural Information Processing Systems*. 6604–6615.
- [25] Dan Hendrycks and Thomas Dietterich. 2019. Benchmarking neural network robustness to common corruptions and perturbations. *arXiv preprint arXiv:1903.12261* (2019).
- [26] Kevin Jarrett, Koray Kavukcuoglu, Marc'Aurelio Ranzato, and Yann LeCun. 2009. What is the best multi-stage architecture for object recognition?. In *2009 IEEE 12th international conference on computer vision*. IEEE, 2146–2153.
- [27] Jinyuan Jia, Ahmed Salem, Michael Backes, Yang Zhang, and Neil Zhenqiang Gong. 2019. Memguard: Defending against black-box membership inference attacks via adversarial examples. In *Proceedings of the 2019 ACM SIGSAC Conference on Computer and Communications Security*. 259–274.
- [28] Daniel Kifer, Adam Smith, and Abhradeep Thakurta. 2012. Private convex empirical risk minimization and high-dimensional regression. In *Conference on Learning Theory*. 25–1.
- [29] Antti Herman Koskela and Antti Juho Henriikki Honkela. 2018. Learning rate adaptation for differentially private stochastic gradient descent. (2018).
- [30] Alexey Kurakin, Ian Goodfellow, and Samy Bengio. 2016. Adversarial examples in the physical world. *arXiv preprint arXiv:1607.02533* (2016).
- [31] Alexey Kurakin, Ian Goodfellow, and Samy Bengio. 2016. Adversarial machine learning at scale. *arXiv preprint arXiv:1611.01236* (2016).
- [32] Yann LeCun, Léon Bottou, Yoshua Bengio, and Patrick Haffner. 1998. Gradient-based learning applied to document recognition. *Proc. IEEE* 86, 11 (1998), 2278–2324.
- [33] Mathias Lecuyer, Vaggelis Atlidakis, Roxana Geambasu, Daniel Hsu, and Suman Jana. 2019. Certified robustness to adversarial examples with differential privacy. In *2019 IEEE Symposium on Security and Privacy (SP)*. IEEE, 656–672.
- [34] Aleksander Madry, Aleksandar Makelov, Ludwig Schmidt, Dimitris Tsipras, and Adrian Vladu. 2017. Towards deep learning models resistant to adversarial attacks. *arXiv preprint arXiv:1706.06083* (2017).
- [35] Seyed-Mohsen Moosavi-Dezfooli, Alhussein Fawzi, and Pascal Frossard. 2016. Deepfool: a simple and accurate method to fool deep neural networks. In *Proceedings of the IEEE conference on computer vision and pattern recognition*. 2574–2582.
- [36] Seyed-Mohsen Moosavi-Dezfooli, Alhussein Fawzi, Jonathan Uesato, and Pascal Frossard. 2019. Robustness via curvature regularization, and vice versa. In *Proceedings of the IEEE Conference on Computer Vision and Pattern Recognition*. 9078–9086.
- [37] Norman Mu and Justin Gilmer. 2019. Mnist-c: A robustness benchmark for computer vision. *arXiv preprint arXiv:1906.02337* (2019).
- [38] Arvind Narayanan and Vitaly Shmatikov. 2008. Robust de-anonymization of large sparse datasets. In *2008 IEEE Symposium on Security and Privacy (sp 2008)*. IEEE, 111–125.
- [39] Milad Nasr, Reza Shokri, and Amir Houmansadr. 2018. Machine learning with membership privacy using adversarial regularization. In *Proceedings of the 2018 ACM SIGSAC Conference on Computer and Communications Security*. 634–646.
- [40] Arvind Neelakantan, Luke Vilnis, Quoc V Le, Ilya Sutskever, Lukasz Kaiser, Karol Kurach, and James Martens. 2015. Adding gradient noise improves learning for very deep networks. *arXiv preprint arXiv:1511.06807* (2015).

- [41] NhatHai Phan, Ruoming Jin, My T Thai, Han Hu, and Dejing Dou. 2019. Preserving differential privacy in adversarial learning with provable robustness. *arXiv preprint arXiv:1903.09822* (2019).
- [42] Qasim Mahmood Rajpoot and Christian Damsgaard Jensen. 2014. Security and privacy in video surveillance: Requirements and challenges. In *IFIP International Information Security Conference*. Springer, 169–184.
- [43] Benjamin IP Rubinstein, Peter L Bartlett, Ling Huang, and Nina Taft. 2009. Learning in a large function space: Privacy-preserving mechanisms for SVM learning. *arXiv preprint arXiv:0911.5708* (2009).
- [44] Mahmood Sharif, Sruti Bhagavatula, Lujo Bauer, and Michael K Reiter. 2016. Accessorize to a crime: Real and stealthy attacks on state-of-the-art face recognition. In *Proceedings of the 2016 acm sigsac conference on computer and communications security*. 1528–1540.
- [45] Reza Shokri and Vitaly Shmatikov. 2015. Privacy-preserving deep learning. In *Proceedings of the 22nd ACM SIGSAC conference on computer and communications security*. 1310–1321.
- [46] Reza Shokri, Marco Stronati, Congzheng Song, and Vitaly Shmatikov. 2017. Membership inference attacks against machine learning models. In *2017 IEEE Symposium on Security and Privacy (SP)*. IEEE, 3–18.
- [47] Congzheng Song, Thomas Ristenpart, and Vitaly Shmatikov. 2017. Machine learning models that remember too much. In *Proceedings of the 2017 ACM SIGSAC Conference on Computer and Communications Security*. 587–601.
- [48] Liwei Song, Reza Shokri, and Prateek Mittal. 2019. Privacy risks of securing machine learning models against adversarial examples. In *Proceedings of the 2019 ACM SIGSAC Conference on Computer and Communications Security*. 241–257.
- [49] Shuang Song, Kamalika Chaudhuri, and Anand D Sarwate. 2013. Stochastic gradient descent with differentially private updates. In *2013 IEEE Global Conference on Signal and Information Processing*. IEEE, 245–248.
- [50] Christian Szegedy, Wojciech Zaremba, Ilya Sutskever, Joan Bruna, Dumitru Erhan, Ian Goodfellow, and Rob Fergus. 2013. Intriguing properties of neural networks. *arXiv preprint arXiv:1312.6199* (2013).
- [51] Florian Tramèr, Fan Zhang, Ari Juels, Michael K Reiter, and Thomas Ristenpart. 2016. Stealing machine learning models via prediction apis. In *25th {USENIX} Security Symposium ({USENIX} Security 16)*. 601–618.
- [52] Binghui Wang and Neil Zhenqiang Gong. 2018. Stealing hyperparameters in machine learning. In *2018 IEEE Symposium on Security and Privacy (SP)*. IEEE, 36–52.
- [53] Samuel Yeom, Irene Giacomelli, Matt Fredrikson, and Somesh Jha. 2018. Privacy risk in machine learning: Analyzing the connection to overfitting. In *2018 IEEE 31st Computer Security Foundations Symposium (CSF)*. IEEE, 268–282.
- [54] Jun Zhang, Zhenjie Zhang, Xiaokui Xiao, Yin Yang, and Marianne Winslett. 2012. Functional mechanism: regression analysis under differential privacy. *arXiv preprint arXiv:1208.0219* (2012).